Comparison of properties and crystalline structures of nitrates, sulphates and phosphates of Co(II) and Ni(II).

Author: Miquel Roda Júlio

Tutor: María Ángeles Tena Gómez

QU0943 – Degree Final Project

Academic course: 2020-21

INDEX

1. INTRODUCTION

The main objective of this project is to compare crystalline properties and structures of nitrates, sulphates and phosphates of Co(II) and Ni(II).

Cobalt (Z = 27) and nickel (Z = 28) are transition metals. They present a valence shell with multiple electrons, cobalt is a d^7 and nickel is a d^8, so they have the ability to give or receive electrons. Moreover, they can also change their oxidation state, being +2 the most common one, but they can also appear in the neutral form (0), +1 and +3. In few compounds, cobalt can present an oxidation state of +4.

When studying the different structures, it is important to remark that they can form multiple polymorphs and appear in different symmetries, so there are plenty of possibilities. For example, phosphates are divided in diphosphates [$M_2P_2O_7$] and orthophosphates [$M_3P_2O_8$].

The studied structures are: trigonal $Co(NO_3)_2$, trigonal $Ni(NO_3)_2$ and cubic $Ni(NO_3)_2$; both α and β-$CoSO_4$ and β-$NiSO_4$; both monoclinic α and β-$Co_2P_2O_7$ and both monoclinic α and β-$Ni_2P_2O_7$; stable $Co_3P_2O_8$ and metastable $Co_3P_2O_8$ and $Ni_3P_2O_8$.

Each structure has particular properties, so the main objective of this paper is to determine which are the most common ones and see how they vary when changing the main ion (Co and Ni) and changing their crystalline structures.

2. CRYSTALLINE STRUCTURES

In both Co(II), d^7, and Ni(II), d^8, the electronic repulsions are important and their characteristics are related with the possibility of cations interaction inside the crystal structure. This interaction increases when the M-M (metal-metal) decreases. In order to highlight the oxygen share of the polyhedrons, we are indicating the minimum value of the metal-metal distance in each of the crystal structures described.

2.1. NITRATES. $M(NO_3)_2$ (M=Co, Ni)

2.1.1. Cobalt (II) nitrate, trigonal $Co(NO_3)_2$

Cobalt (II) nitrate shows a **trigonal symmetry** with **Z = 12** (12 Cobalt atoms in each unity cell). The space group is **R -3 H**, number **148**.

Cell parameters are: a= 10.445(1), b = 10.445(1) and c = 12.769(2); α = 90°, β = 90° and ϒ = 120°.

Atoms are distributed as:

- **Co1**. Co^{+2} in position 9e.
- **Co2**. Co^{+2} in position 3a.
- **N1**. N^{+5} in position 6c, with x = 0.3333, y = 0.6667 and z = 0.0039(11).
- **N2**. N^{+5} in position 18f, with x = 0.2321(9), y = 0.2741(8) and z = 0.1171(6).
- **O1**. O^{-2} in position 18f, with x = 0.3245(8), y = 0.5426(7) and z = 0.0040(6).
- **O2**. O^{-2} in position 18f, with x = 0.2739(8), y = 0.3659(8) and z = 0.1906(6).
- **O3**. O^{-2} in position 18f, with x = 0.1023(7), y = 0.1673(7) and z = 0.1156(6).
- **O4**. O^{-2} in position 18f, with x = 0.3209(8), y = 0.2895(8) and z = 0.0458(6).

In this structure, the Co(II) ions occupy octahedral positions. Isolated octahedra are bound by nitrate ions. The minimum Metal-Metal distance is: 5.244 Å

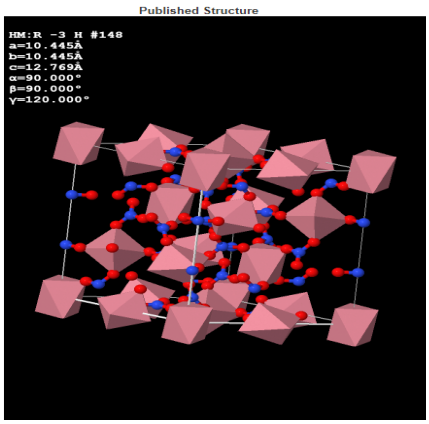

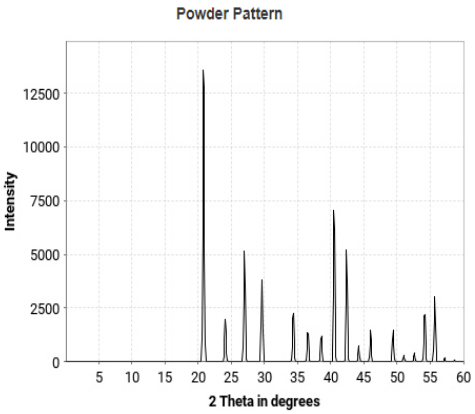

ICSD – 189915 [1]

2.1.2. Nickel (II) nitrate, trigonal $Ni(NO_3)_2$

Nickel (II) nitrate shows a **trigonal symmetry** with **Z = 12** (12 Nickel atoms in each unity cell). The space group is **R -3 H**, number **148**.

Cell parameters are: a = 10.332(1), b = 10.332(1) and c = 12.658(2); α = 90°, β = 90° and ϒ = 120°.

Atoms are distributed as:

- **Ni1.** Ni^{+2} in position 9e.
- **Ni2.** Ni^{+2} in position 3a.
- **N1**. N^{+5} in position 6c, with x = 0.3333, y = 0.6667 and z = 0.0011(14).
- **N2**. N^{+5} in position 18f, with x = 0.2313(12), y = 0.2750(12) and z = 0.1166(8).
- **O1**. O^{-2} in position 18f, with x = 0.3259(10), y = 0.5420(10) and z = 0.0011(7).
- **O2**. O^{-2} in position 18f, with x = 0.2722(11), y = 0.3671(10) and z = 0.1913(7).
- **O3**. O^{-2} in position 18f, with x = 0.0999(10), y = 0.1677(10) and z = 0.1133(7).
- **O4**. O^{-2} in position 18f, with x = 0.3230(11), y = 0.2913(11) and z = 0.0458(8).

In this structure, the Ni(II) ions occupy octahedral positions. Isolated octahedra are bound by nitrate ions. The minimum Metal-Metal distance is: 5.166 Å

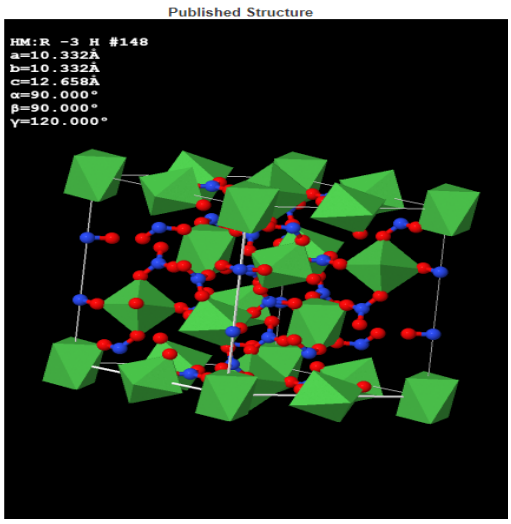

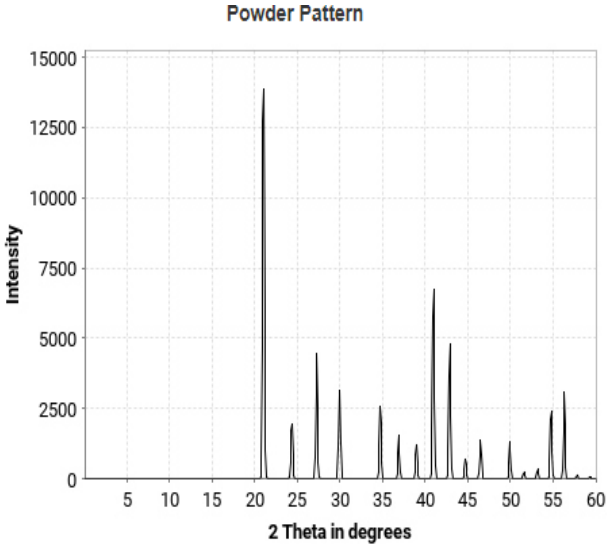

ICSD – 189916 [1]

2.1.3. Nickel(II) nitrate. Cubic $Ni(NO_3)_2$

Nickel (II) nitrate shows a **cubic symmetry** with **Z = 4** (4 Nickel atoms in each unity cell). The space group is **P a -3**, number **205**.

Cell parameters are: a = 7.31, b = 7.31 and c = 7.31; α = 90°, β = 90° and ϒ = 90°.

Atoms are distributed as:

- **Ni1.** Ni^{+2} in position 4a.
- **N1**. N^{+5} in position 8c, with x = 0.338, y = 0.338 and z = 0.338.
- **O1**. O^{-2} in position 24d, with x = 0.245, y = 0.28 and z = 0.467.

In this structure, the Ni(II) ions occupy octahedral positions. Isolated octahedra are bound by nitrate ions. The minimum Metal-Metal distance is: 5.169 Å

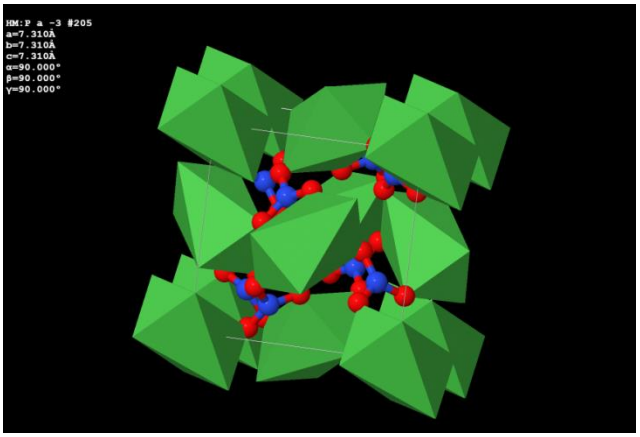
HM:P a -3 #205
a=7.310Å
b=7.310Å
c=7.310Å
α=90.000°
β=90.000°
γ=90.000°

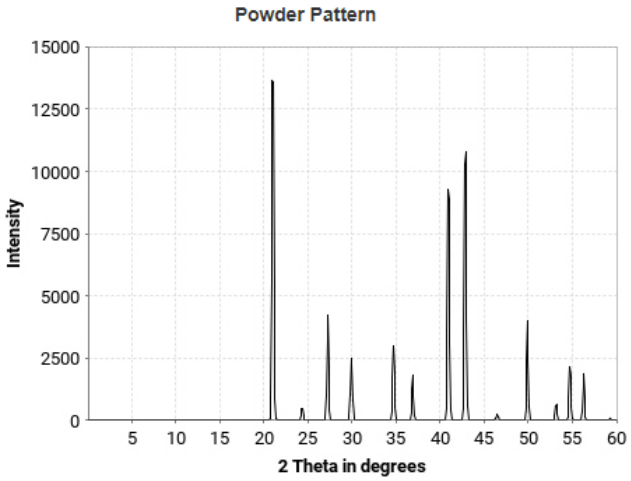
Powder Pattern
Intensity
15000
12500
10000
7500
5000
2500
0
5
10
15
20
25
30
35
40
45
50
55
60
2 Theta in degrees

ICSD – 28327 [1]

2.2. SULPHATES. MSO_4 (M=Co, Ni)

2.2.1. Cobalt (II) sulphate, β-$CoSO_4$

β-Cobalt (II) sulphate shows an **orthorhombic symmetry** with **Z = 4** (4 Cobalt atoms in each unity cell). The space group is **C m c m**, number **63**.

Cell parameters are: a = 5.192(1), b = 7.856(2) and c = 6.530(2); α = 90º, β = 90º and ϒ = 90º.

Atoms are distributed as:

- **Co1.** Co^{+2} in position 4a.
- **S1.** S^{+6} in position 4c, with y = 0.3523(1).
- **O1.** O^{-2} in position 8f, with y = 0.2513(2) and z = 0.0627(2).
- **O2.** O^{-2} in position 8g, with x = 0.2342(3) and y = 0.4633(2).

In this structure, the Co(II) ions occupy octahedral positions. The octahedra share edges forming chains of octahedra. Chains are linked by sulphate ions. The minimum Metal-Metal distance is: 3.286 Å.

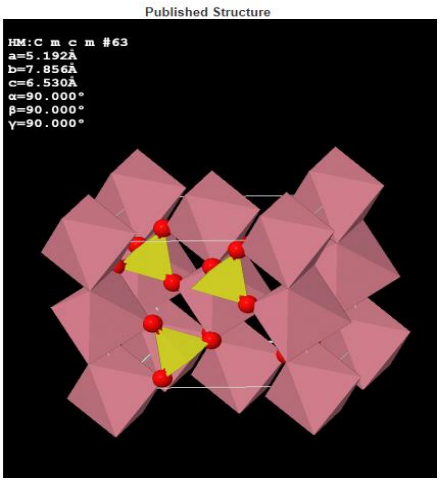

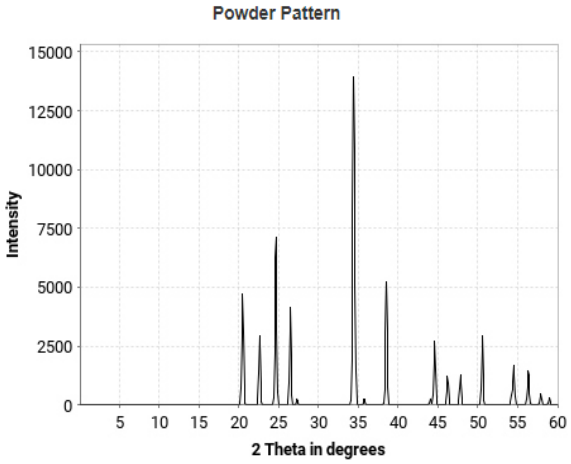

ICSD – 33736 [1]

2.2.2. Cobalt (II) sulphate, α-$CoSO_4$

α-Cobalt (II) sulphate shows an **orthorhombic symmetry** with **Z = 4** (4 Cobalt atoms in each unity cell). The space group is **P n m a**, number **62**.

Cell parameters are: a = 8.6127(4), b = 6.7058(3) and c = 4.7399(2); α = 90º, β = 90º and ϒ = 90º.

Atoms are distributed as:

- **Co1.** Co^{+2} in position 4a.
- **S1.** S^{+6} in position 4c, with x = 0.1795(4) and z = 0.4740(11).
- **O1.** O^{-2} in position 4c, with x = 0.1267(12) and z = 0.7729(19).
- **O2.** O^{-2} in position 4c, with x = 0.3547(10) and z = 0.4506(19).
- **O3**. O^{-2} in position 8d, with x = 0.1287(7), y = 0.0648(10) and z = 0.3413(12).

In this structure, the Co(II) ions occupy octahedral positions. The octahedra share edges forming chains of octahedra. Chains are linked by sulphate ions. The minimum Metal-Metal distance is: 3.353 Å.

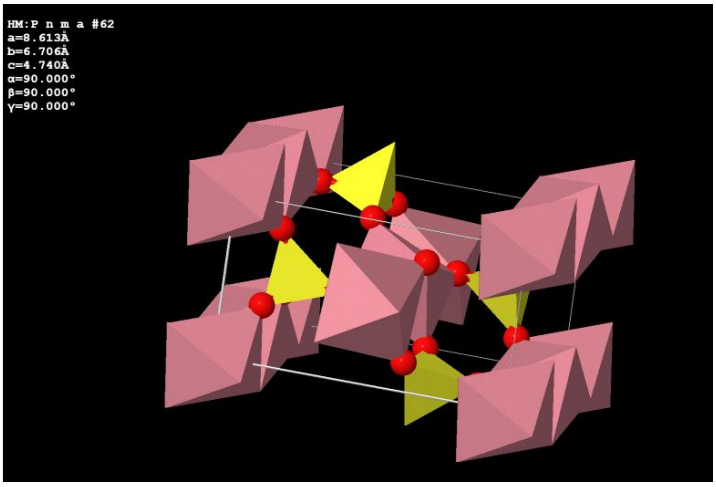

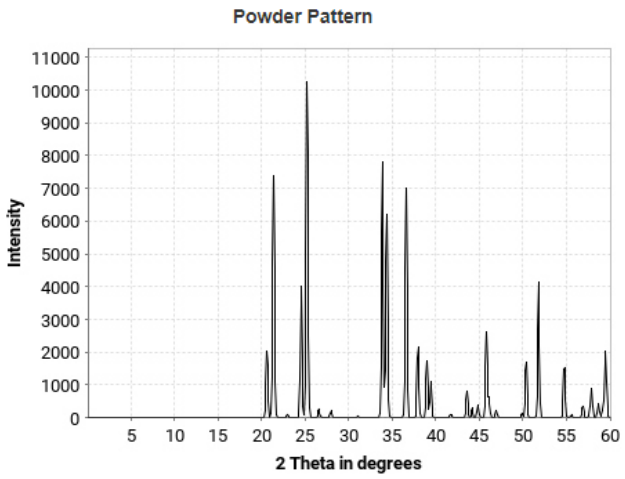

ICSD – 74161 [1]

2.2.3. Nickel (II) sulphate, β-$NiSO_4$

β-Nickel (II) sulphate shows an **orthorhombic symmetry** with **Z = 4** (4 Nickel atoms in each unity cell). The space group is **C m c m**, number **63**.

Cell parameters are: a = 5.166(1), b = 7.846(2) and c = 6.362(2); α = 90º, β = 90º and ϒ = 90º.

Atoms are distributed as:

- **Ni1**. Ni^{+2} in position 4a.
- **S1.** S^{+6} in position 4c, with y = 0.3527(4).
- **O1**. O^{-2} in position 8f, with y = 0.2531(6) and z = 0.0579(6).
- **O2**. O^{-2} in position 8g, with x = 0.2344(7) and y = 0.4654(6).

In this structure, the Ni(II) ions occupy octahedral positions. The octahedra share edges forming chains of octahedra. Chains are linked by sulphate ions. The minimum Metal-Metal distance is: 3.181 Å

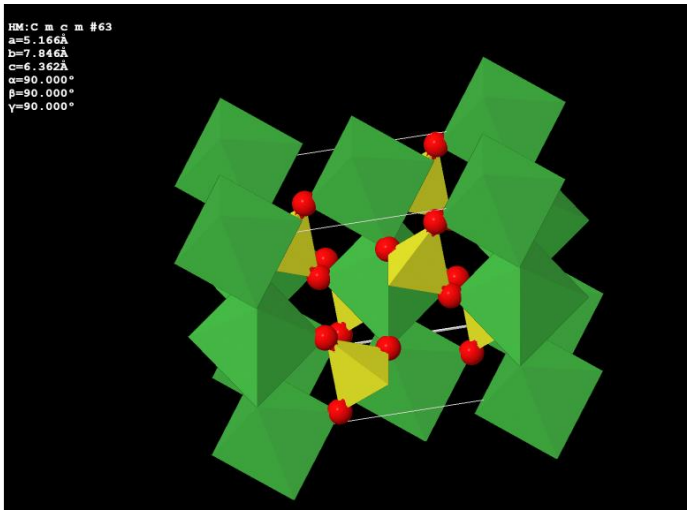

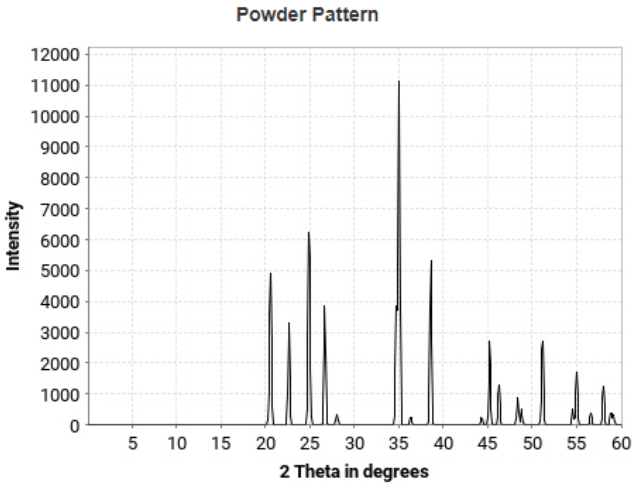

ICSD – 33737 [1]

2.3. DIPHOSPHATES. $M_2P_2O_7$ (M=Co, Ni)

2.3.1. Cobalt (II) diphosphate, monoclinic α-$Co_2P_2O_7$.

α-Cobalt(II) diphosphate shows a **monoclinic symmetry** with **Z = 2** (2 Cobalt atoms in each unity cell). The space group is **P 1 21/a 1**, number **14**.

Cell parameters are: a = 5.339(1), b = 9.923(1) and c = 4.488(1); α = 90º, β = 90.45(2)º and ϒ = 90º.

Atoms are distributed as:

- **Co1.** Co^{+2} in position 4e, with x = 0.0897(1), y = 0.1575(1) and z = 0.3929(2).
- **P1.** P^{+5} in position 4e, with x = 0.6543(2), y = 0.1104(1) and z = 0.8558(3).
- **O1.** O^{-2} in position 4e, with x = 0.7603(6), y = 0.2015(4) and z = 0.1125(9).
- **O2.** O^{-2} in position 4e, with x = 0.8616(6), y = 0.0394(4) and z = 0.7102(9).
- **O3.** O^{-2} in position 4e, with x = 0.4681(7), y = 0.1807(3) and z = 0.6220(8).
- **O4.** O^{-2} in position 2c.

In this structure, the Co(II) ions occupy octahedral positions and square-based pyramid positions. The octahedra share edges with the square-based pyramids. Each octahedron is also linked to PO_4 tetrahedra. The minimum Metal-Metal distance is: 3.166 Å.

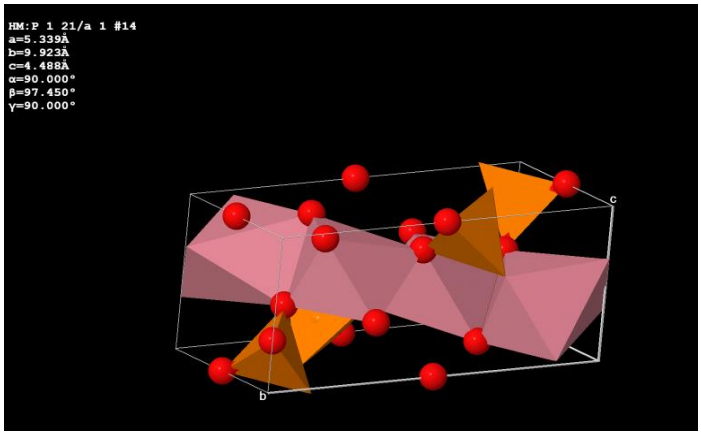

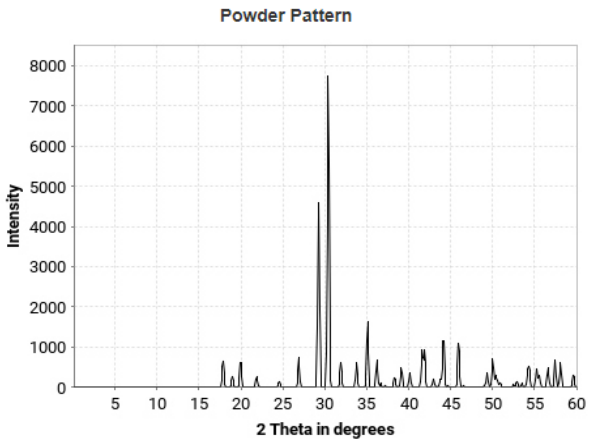

ICSD – 59291 [1]

2.3.2. Cobalt (II) diphosphate, monoclinic β-$Co_2P_2O_7$

β-Cobalt (II) diphosphate shows a **monoclinic symmetry** with **Z = 2** (2 Cobalt atoms in each unity cell). The space group is **A 1 2/m 1**, number **12.**

Cell parameters are: a = 4.524(2), b = 8.526(4) and c = 6.640(3); α = 90º, β = 102.59(3)º and ϒ = 90º.

Atoms are distributed as:

- **Co1**. Co^{+2} in position 4h, with y = 0.6926(2).
- **P1**. P^{+5} in position 4i, with x = -0.088(8), y = 0.5 and z = 0.7160(6).
- **O1**. O^{-2} in position 4i, with x = 0.214(3) and z = 0.369(2).
- **O2.** O^{-2} in position 8j, with x = 0.728(2), y = 0.648(1) and z = 0.725(2).
- **O3.** O^{-2} in position 2a.

In this structure, the Co (II) ions occupy octahedral positions. Octahedra are distributed in layers joined by PO_4 tetrahedra. The minimum Metal-Metal distance is: 3.264 Å.

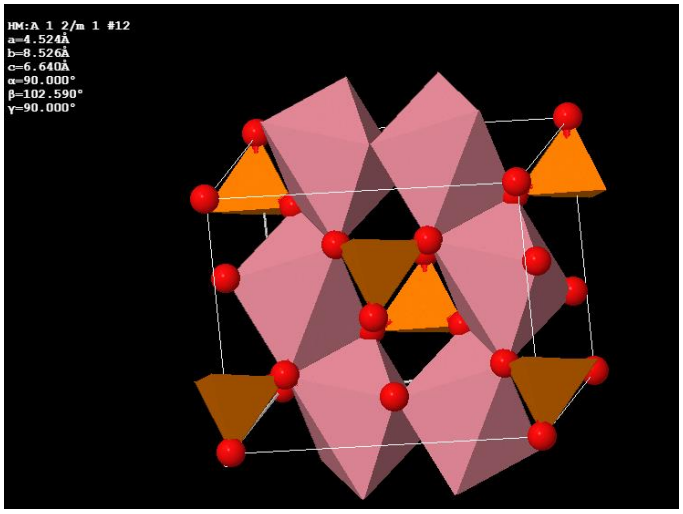

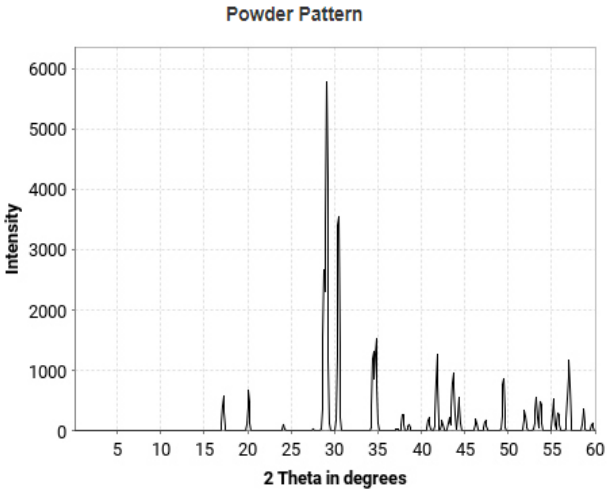

ICSD – 74542 [1]

2.3.3. Nickel (II) diphosphate, monoclinic β-$Ni_2P_2O_7$

β-Nickel (II) diphosphate shows a **monoclinic symmetry** with **Z = 2** (2 Nickel atoms in each unity cell). The space group is **C 1 2/m 1**, number **12**.

Cell parameters are: a = 6.501, b = 8.239 and c = 4.480; α = 90º, β = 104.14º and ϒ = 90º.

Atoms are distributed as:

- **Ni1.** Ni^{+2} in position 4h, with y = 0.310(1).
- **P1.** P^{+5} in position 4i, with x = 0.210(1) and z = 0.908(2).
- **O1.** O^{-2} in position 2a.
- **O2.** O^{-2} in position 4i, with x = 0.387(4) and z = 0.220(7).
- **O3.** O^{-2} in position 8j, with x = 0.218(3), y = 0.151(4) and z = 0.721(5).

In this structure, the Ni (II) ions occupy octahedral positions. Octahedra are distributed in layers joined by PO_4 tetrahedra. The minimum metal-to-metal distance is: 3.131 Å

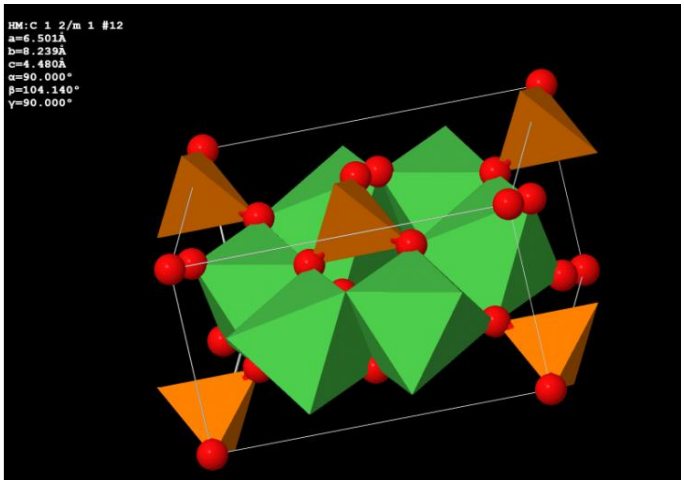

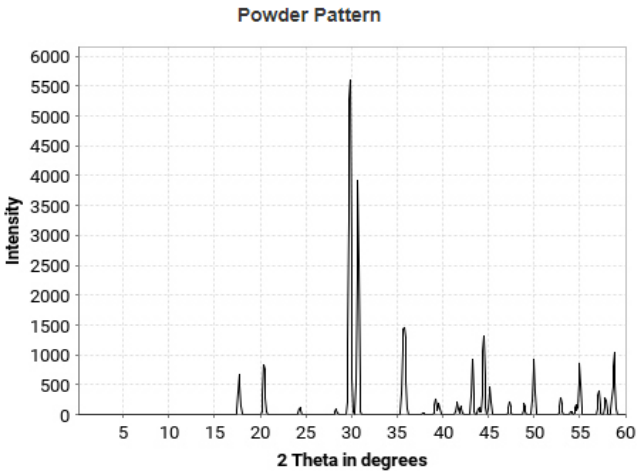

ICSD – 30433 [1]

2.3.4. Nickel (II) diphosphate, monoclinic α-$Ni_2P_2O_7$

α-Nickel (II) diphosphate shows a **monoclinic symmetry** with **Z = 2** (2 Nickel atoms in each cell unity). The space group is **P 1 21/a 1**, number **14.**

Cell parameters are: a = 5.212(3), b = 9.913(5) and c = 4.475(3); α = 90º, β = 97.46(10)º and ϒ = 90º.

Atoms are distributed as:

- **Ni1**. Ni^{+2} in position 4e, with x = 0.5841(6), y = 0.3434(3) and z = 0.9034(7).
- **P1.** P^{+5} in position 4e, with x = 0.6569(1), y = 0.1113(6) and z = 0.3579(1).
- **O1**. O^{-2} in position 4e, with x = 0.7618(3), y = 0.2037(2) and z = 0.6177(4).
- **O2**. O^{-2} in position 4e, with x = 0.4635(4), y = 0.1793(2) and z = 0.1194(4).
- **O3.** O^{-2} in position 4e, with x = 0.8713(4), y = 0.0415(2) and z = 0.2132(4).
- **O4**. O^{-2} in position 2b.

In this structure, the Co (II) ions occupy octahedral positions. Octahedra are distributed in layers joined by PO_4 tetrahedra. The minimum metal-to-metal distance is: 3.197 Å.

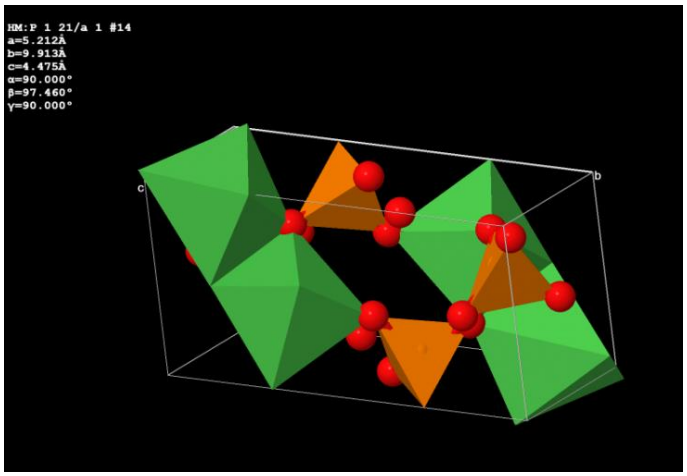

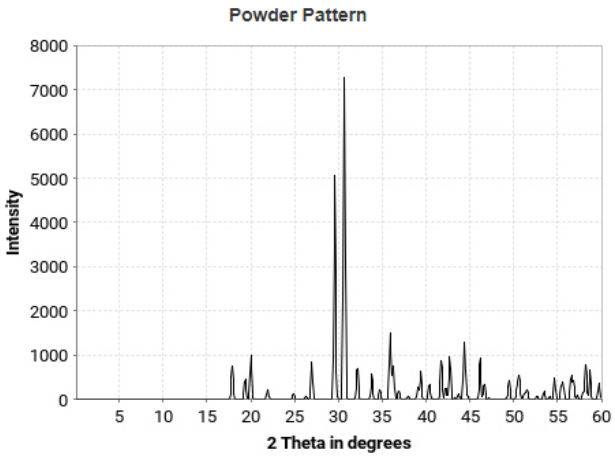

ICSD – 100194 [1]

2.4. ORTHOPHOSPHATES $M_3P_2O_8$ (M=Co, Ni).

2.4.1. Cobalt (II) orthophosphate, stable $Co_3P_2O_8$

Stable cobalt (II) orthophosphate shows a **monoclinic symmetry** with **Z = 2** (2 Cobalt atoms in each unity cell). The space group is **P 1 21/c 1**, number **14**.

Cell parameters are: a = 5.063(2), b = 8.361(2) and c = 8.788(2); α = 90º, β = 121.00(2)º and ϒ = 90º.

Atoms are distributed as:

- **Co1**. Co^{+2} in position 2a.
- **Co2.** Co^{+2} in position 4e, with x = 0.0202(1), y = 0.3591(1) and z = 0.1142(1).
- **P1**. P^{+5} in position 4e, with x = 0.3404(2), y = 0.6938(1) and z = 0.3024(1).
- **O1**. O^{-2} in position 4e, with x = 0.2729(6), y = 0.6422(3) and z = 0.4455(4).
- **O2**. O^{-2} in position 4e, with x = 0.6881(6), y = 0.6958(3) and z = 0.3750(3).
- **O3**. O^{-2} in position 4e, with x = 0.1902(6), y = 0.5786(3) and z = 0.1432(4).
- **O4**. O^{-2} in position 4e, with x = 0.1903(6), y = 0.8618(3) and z = 0.2435(4).

In this structure, the Co(II) ions occupy octahedral positions and square-based pyramid positions distributed in layers and joined by PO_4 tetrahedra. The minimum metal-to-metal distance is: 3.148 Å.

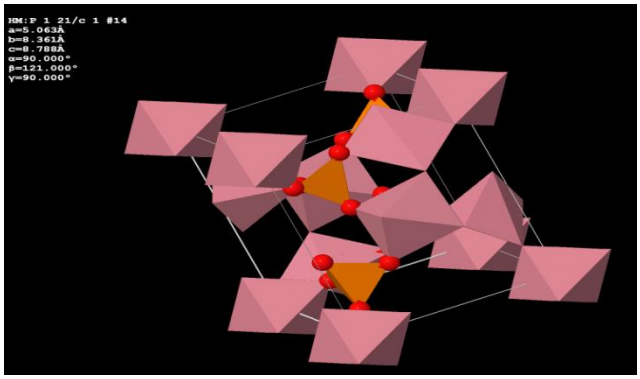

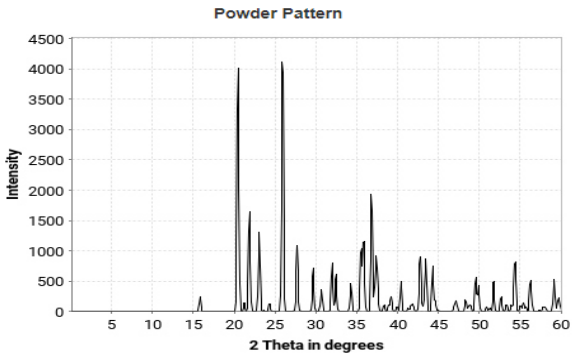

ICSD – 4268 [1]

2.4.2. Cobalt (II) orthophosphate, metastable $Co_3P_2O_8$

Metastable cobalt (II) orthophosphate shows **monoclinic symmetry** with **Z = 2** (2 Cobalt atoms in each unity cell). The space group is **P 1 1 21/b**, number **14**.

Cell parameters are: a = 5.92(2), b = 10.334(30) and c = 4.75(2); α = 90º, β = 90(2)º and ϒ = 91.07º.

Atoms are distributed as:

- **Co1**. Co^{+2} in position 2d.
- **Co2.** Co^{+2} in position 4e, with x = 0.227(8), y = 0.778(8) and z = 0.483(8).
- **P1**. P^{+5} in position 4e, with x = 0.277(8), y = 0.100(8) and z = 0.430(8).
- **O1**. O^{-2} in position 4e, with x = 0.279(8), y = 0.581(8) and z = 0.242(8).
- **O2**. O^{-2} in position 4e, with x = 0.246(8), y = 0.462(8) and z = 0.193(8).
- **O3**. O^{-2} in position 4e, with x = 0.096(8), y = 0.168(8) and z = 0.298(8).
- **O4**. O^{-2} in position 4e, with x = 0.493(8), y = 0.139(8) and z = 0.258(8).

In this structure, all of the Co (II) ions occupy octahedral positions. Octahedra are three-dimensionally distributed and linked by PO_4 tetrahedra. The minimum metal-to-metal distance is: 3.323 Å.

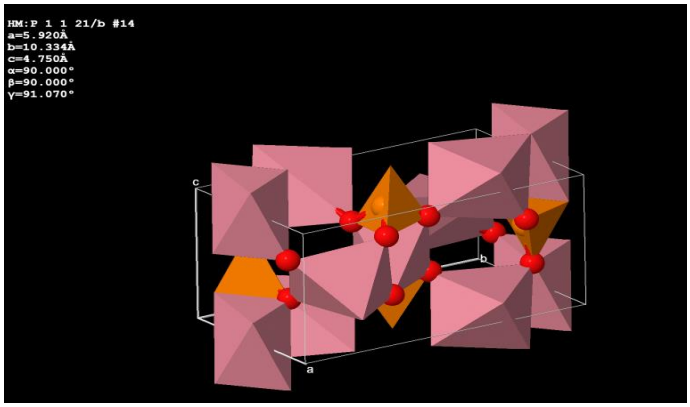

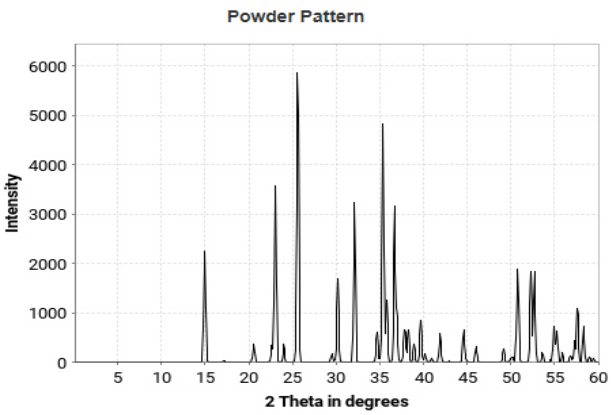

ICSD – 9850 [1]

2.4.3. Nickel (II) orthophosphate, $Ni_3P_2O_8$

Nickel (II) orthophosphate shows a **monoclinic symmetry** with **Z = 2** (2 Nickel atoms in each unity cell). The space group is **P 1 21/c 1**, number **14**.

Cell parameters are: a = 5.824(1), b = 4.694(1) and c = 10.101(1); α = 90º, β = 91.134(1)º and ϒ = 90º.

Atoms are distributed as:

- **Ni1.** Ni^{+2} in position 2b.
- **Ni2.** Ni^{+2} in position 4e, with x = 0.2416(2), y = 0.4855(2) and z = 0.7746(1).
- **P1**. P^{+5} in position 4e, with x = 0.2500(3), y = 0.4222(2) and z = 0.0945(2).
- **O1.** O^{-2} in position 4e, with x = 0.2667(3), y = 0.7466(3) and z = 0.1019(2).
- **O2.** O^{-2} in position 4e, with x = 0.2566(3), y = 0.1928(3) and z = 0.4517(2).
- **O3.** O^{-2} in position 4e, with x = 0.0507(3), y = 0.3003(3) and z = 0.1729(2).
- **O4**. O^{-2} in position 4e, with x = 0.4655(3), y = 0.2651(4) and z = 0.1621(2).

In this structure, all of the Ni(II) ions occupy octahedral positions. Octahedra are three-dimensionally distributed and linked by PO_4 tetrahedra. The minimum metal-to-metal distance is: 3.113 Å.

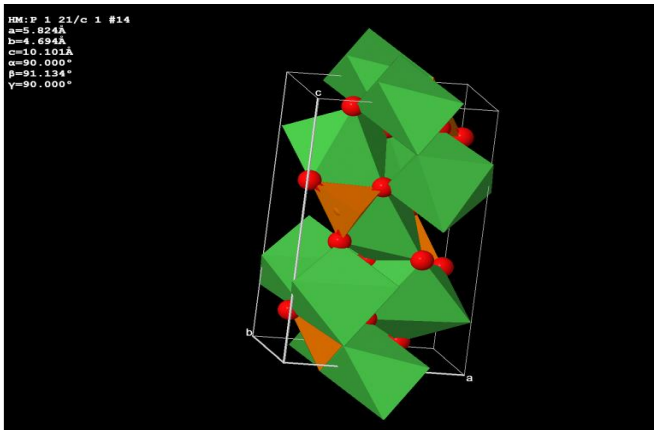

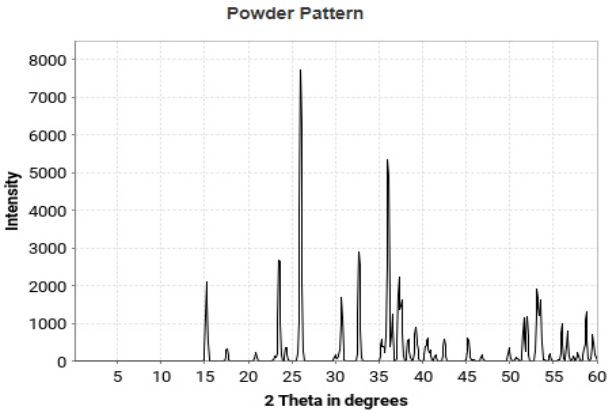

ICSD – 4268 [1]

3. PROPERTIES

3.1. Catalytic activity and thermal decomposition

The low decomposition temperatures of nitrates generating the gas phase, which lowers temperature of formation of compounds with the metal ions that are part of these nitrates. The products obtained in thermal decomposition are used in many cases as catalysts.
A catalyst is a simple or compound chemical substance that modifies the speed of a chemical reaction, intervening in it but without becoming part of the resulting products [2].

Catalysts have the ability to alter the rate of the reaction without making a change in the thermodynamic properties of the reaction. Both Cobalt (Z = 27, d^7) and Nickel (Z = 28, d^8) have a major impact in catalyst compounds. The main reason is that they are transition metals, so they present lots of electrons in the valence shell (d-orbital), but also many places that are not occupied. Because of this, they can lend or withdraw electrons from the reagent. Moreover, they can interchange their oxidation state, so they can form complexes with the reagents.

Nitrates

Anhydrous transition metal nitrates and their hydrates are widely used for preparation of catalyst materials such as oxides and metals [3].

Metal nitrates are most popular precursor components for the preparation of oxidic and metallic materials with wide spread properties as high surface catalysts, ceramics, semiconductors, gas sensors and high temperature superconductors [3]. Especially, cobalt and alumina supported cobalt oxide catalysts have been widely applied in Fischer-Tropsch synthesis, hydrocracking and selective hydrogenation reactions. The Fischer–Tropsch synthesis involves the conversion of carbon monoxide and hydrogen to predominantly hydrocarbon products, either olefins or paraffins [4]. The main use of nickel nitrate is in the production of catalysts, especially sulphur sensitive catalysts, and as an intermediate in the production of nickel-cadmium batteries. Nickel nitrate is also used to make products used in the pre-treatment of metals prior to painting and prior to cold-forming processes.

Like other nitrates, nickel nitrate is oxidizing, so that caution should be exercised when it contacts with reducing materials such as organic substances [5].

Especially thermogravimetry (TG) in its quasi-isothermal variant is a very helpful tool for the study of decomposition reactions in combination with structure sensitive methods as, Raman and IR spectroscopy and X-ray diffraction measurements [4].

The actual decomposition processes often depend very much upon the experimental conditions employed as for example heating rate, amount and packing of starting material, kind and pressure of the gas atmosphere, gas flow rate, melting/formation of a hydrate melt, and others more [3].

The very slow thermal decomposition of cobalt(II) nitrate hexahydrate, reveals the stepwise formation of distinct hydrates as tetra- and di-hydrate, respectively, and of anhydrous cobalt(II)nitrate as a pink coloured product. To elucidate the unusual quasi-isothermal driving modus of the investigation method exemplarily the time dependence on the mass loss and on the temperature. The used atmosphere (N_2 or H_2/N_2) has no influence for the dehy-dration steps. The further thermal decomposition of cobalt(II) nitrate anhydrous results in the formation of the cobalt oxides Co_2O_3 and Co_3O_4 in N_2 atmosphere, whereas in H_2/N_2 finally metallic cobalt is generated [4].

Rapid heating of $Co(NO_3)_2$ causes the formation of a hydrate melt changing the system drastically by incoupled side reactions and evaporation of HNO_3 and other volatile species. This might be the main reason for the quite differing results and findings of the thermal $Co(NO_3)_2{\cdot}6H_2O$ decomposition and also for its non-reproducibility. Another error source of the mentioned decomposition is eventually the formation of cobalt(III) oxonitrate by the reaction of leaving water with dense packed sample material. For further cobalt(II) nitrate decomposition at higher temperatures, the atmosphere is important, whereas in N_2 Co_3O_4 and in H_2/N_2 metallic cobalt is formed [4].

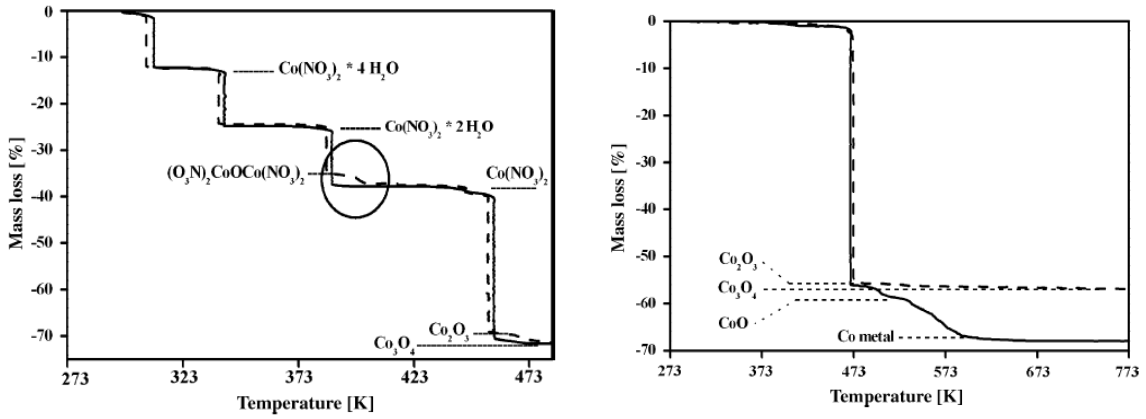

Figure 1. On the left, thermal decomposition of cobalt(II) nitrate hexahydrate. On the right, the thermal decomposition of anhydrous cobalt(II) nitrate [3].

Table 1. Reactions that take place during the thermal decomposition of cobalt(II) nitrate hexahydrate [3].

Reaction/step	T (K)[a]	Δm (%)[b]		Atmosphere
		Experimental	Calculated	
(1) $Co(NO_3)_2{\cdot}6H_2O \rightarrow Co(NO_3)_2{\cdot}4H_2O + 2H_2O$	~308	12.3	12.38	N_2; H_2/N_2
(2) $Co(NO_3)_2{\cdot}4H_2O \rightarrow Co(NO_3)_2{\cdot}2H_2O + 2H_2O$	~340	24.8	24.75	N_2; H_2/N_2
(3) $Co(NO_3)_2{\cdot}2H_2O \rightarrow Co(NO_3)_2 + 2H_2O$	~383	37.5	37.12	N_2; H_2/N_2
(3a) Possible side reaction[c], $2Co(NO_3)_2{\cdot}2H_2O \rightarrow [Co(NO_3)_2]_2O + H_2 + 3H_2O$	~385	34.7	34.37	N_2; H_2/N_2
(3b) $[Co(NO_3)_2]_2O \rightarrow 2Co(NO_3)_2 + 1/2O_2$	~398	37.5	37.12	N_2; H_2/N_2
(4a) $2Co(NO_3)_2 \rightarrow Co_2O_3 + N_2O_4 + N_2O_5$	~458[d]	71.0	71.50	N_2; H_2/N_2
(4b) $3Co(NO_3)_2 \rightarrow Co_3O_4 + N_2O_4 + 2N_2O_5$		72.4	72.20	
(5a) $Co_2O_3 + 3H_2 \rightarrow 2Co + 3H_2O$	~458[d]		Fig. 3	H_2/N_2
(5b) $Co_3O_4 + 4H_2 \rightarrow 3Co + 4H_2O$				
(6) $NO[Co(NO_3)_3] \rightarrow Co(NO_3)_2 + 2NO_2$	~343	33.5	33.46	N_2 (Fig. 4)

In general it is agreed that the thermal degradation/decomposition of nickel(II) nitrate hexahydrate proceeds stepwise and the distinct tetra- and dihydrates are formed if melting respective formation of a hydrate melt (m.p. 56.7 ◦C) is prevented. Besides this, recently a proof of the existence of the controversial intermediate nickel nitrate salt $Ni(NO_3)_2{\cdot}5.5H_2O$ is claimed. Noteworthy, the third degradation step of the nickel compound differs from this of the cobalt homologue and it results in basic species, and not in anhydrous $Ni(NO_3)_2$. The statements for the composition of such basic products differ. A homogenous single phase $Ni_3(NO_3)_2(OH)_4$ could be characterised recently. The formation of the mentioned basic nickel salt corresponds to an hydrolysis of nitrate and the release of HNO_3 [3].

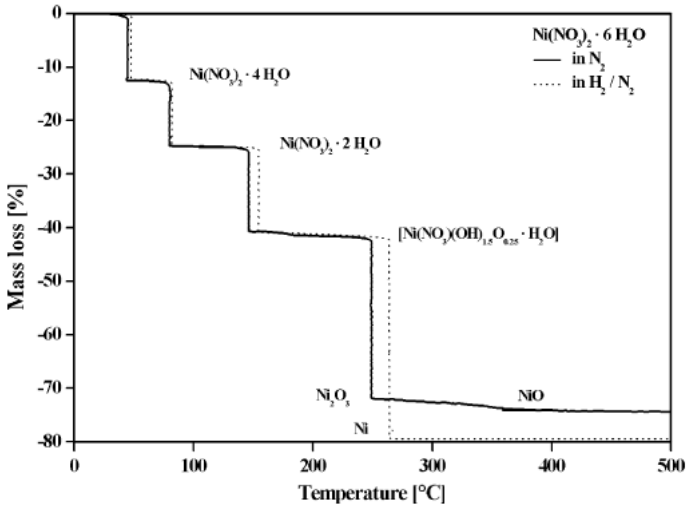

Figure 2. Thermal decomposition of nickel(II) nitrate hexahydrate [3].

Table 2. Reactions that take place during the thermal decomposition of nickel(II) nitrate hexahydrate [3].

Reaction/step	T (K)[a]	Δm (%)[b]	
		Experimental	(Calculated)
Water separation			
1. $Ni(NO_3)_2{\cdot}6H_2O = Ni(NO_3)_2{\cdot}4H_2O + 2H_2O$	316	12.3	(12.38)
2. $Ni(NO_3)_2{\cdot}4H_2O = Ni(NO_3)_2{\cdot}2H_2O + 2H_2O$	353	24.8	(24.77)
Partial decomposition steps (oxidation and partial condensation)			
3a. $Ni(NO_3)_2{\cdot}2H_2O = Ni(NO_3)(OH)_2{\cdot}H_2O + NO_2$	418	40.6	(40.59)
3b. $Ni(NO_3)(OH)_2{\cdot}H_2O = Ni(NO_3)(OH)_{1.5}O_{0.25}{\cdot}H_2O + 0.25H_2O$	~463	42.0	(42.14)
Decomposition			
4. $Ni(NO_3)(OH)_{1.5}O_{0.25}{\cdot}H_2O = 0.5Ni_2O_3 + HNO_3 + 1.25H_2O$	523	71.8	(71.55)
Oxide decomposition to "NiO"			
5. $3Ni_2O_3 = 2Ni_3O_4 + 0.5O_2$	~523[c]	72.2	(72.47)
6. $Ni_3O_4 = 3NiO + 0.5O_2$	~573[c]	74.0	(74.31)
Reduction with H_2/N_2 (10% H_2) to Ni, from 4			
$3NiO + 3/2H_2 = 3Ni + 3/2H_2O$ (Fig. 3)	~535	79.8	(79.81)

Contrary to the calcium and cobalt nitrate hydrates, the thermal dehydration/decomposition of $Ni(NO_3)_2 \cdot 6H_2O$ does not lead to anhydrous $Ni(NO_3)_2$, instead basic intermediate products are formed. In the relevant composition range no distinct phases could be characterised by X-ray diffraction. Therefore, the reaction mechanism of the thermal decomposition of $Ni(NO_3)_2 \cdot 2H_2O$ to basic intermediates either by hydrolysis of nitrate ion or by redox reactions is finally unproved. For further decomposition at higher temperatures the used atmosphere is important, whereas in N_2 nickel oxides and in H_2/N_2 (10% H_2) elemental nickel are formed [3].

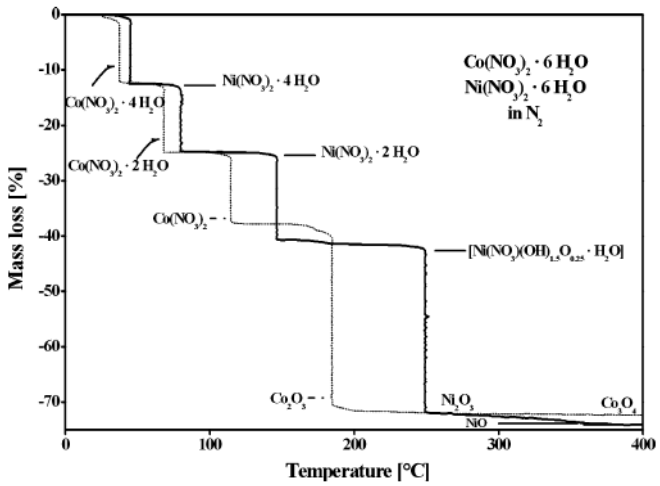

Figure 3. Comparison between the thermal decomposition of nickel and cobalt precursors [3].

In case of the thermal decomposition of Cobalt (II) and Nickel (II) nitrates precursors, they both show a similar first weight loss step, which is attributed to the water loss. As expected, the increase of temperature leads to anhydrous cobalt (II) nitrate, however nickel (II) nitrate follows different rules, and the last degradation step results in basic species, not in anhydrous nickel (II) nitrate. The formation of this basic intermediate might be caused by an hydrolysis of nitrate and the release of HNO_3 or because redox reactions interfering the process. Never the less, it is not clear why nickel nitrate has this different behaviour and more studies are needed in the future.

Orthophosphates

The electrocatalytic activity of the synthesized $Ni_xCo_{3-x}(PO_4)_2$ samples toward the OER (Oxygen Evolution Reaction) and ORR (Oxygen Reduction Reaction) was studied in an aqueous 0.1 M NaOH electrolyte. In general, the OER is the primary charging reaction in the air electrode of metal-air batteries. However, the reaction is kinetically sluggish due to the involvement of multielectron steps with several intermediates. Therefore, the OER usually requires a large overpotential, which necessitates the use of highly active catalysts [6]. The catalyst helps in reducing the required overpotential and thus improving the voltaic and round-trip efficiency of the battery. The catalyst should also be stable in the electrolyte under the harsh oxidative potential of the OER to provide sufficient battery lifetime. It is reported that the adsorption/desorption energies of the reaction intermediates largely determine the OER kinetic overpotentials. An ideal catalyst has optimum binding energy for the intermediates, which is neither too strong nor too week, resulting in a volcano-shaped correlation between activity and binding energy [6]. Doping of foreign metal ions is a generally used strategy to finely tune the electronic properties, morphologies, and adsorption energies to improve the OER kinetics. Hence, it is anticipated that the bimetallic catalyst with an optimum metal-ion ratio can offer high electronic conductivity, surface area, an ideal value for the adsorption energy, etc., which will result in high OER activity. The cobalt phosphate (CP) material shows the least OER catalytic activity with an overpotential of 493 mV. Nickel phosphate (NP) shows slightly higher activity and requires 26 mV less overpotential for the same current [6].

All bimetallic phosphate catalysts (NCP) exhibit superior performance to monometallic catalysts [6]. The OER activity follows the order NCP11 ($Ni_{1.5}Co_{1.5}(PO_4)_2$) > NP > CP. The best catalyst NCP11 requires an overpotential of 340 mV at 4.8 mA cm^{-2}, which is 153 and 127 mV lower than those of CP and NP, respectively. This clearly indicates the advantage of incorporating both the metal ions in the same material. It is to be noted that the overpotential for 10 mA cm^{-2} is the generally used standard for comparing the OER performance of different catalysts [6].

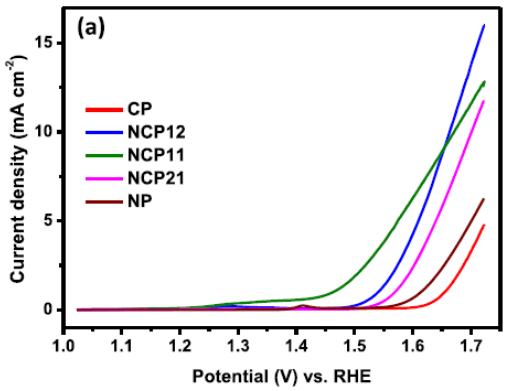

Figure 4. Catalytic activity of diphosphates and monophosphates [6].

Cobalt orthophosphate forms a hydrated structure up to 700 °C. Hence, the combustion-synthesized foamy powders were calcined at 800 °C for 5 hours to get a fully dehydrated phase [6].

The themogravimetric analysis (TGA) curve of Ni(II) orthophosphate shows two weight loss processes: the first weight loss between 100 and 200 °C is due to removal of water molecules, and the corresponding endothermic peak is observed at 180 °C. The second weight loss is due to the exothermic combustion reactions involving emission of CO_2 and NO_2 gases. The exothermic peak centred at 300 °C stems from the combustion process [6].

Diphosphates

In the TG curve of $Co_2P_2O_7 \cdot 6H_2O$, the weight loss can be divided into two stages. All the endotherms peaks in the DSC curve are considered to result from the removal of water molecules from the structure of $Co_2P_2O_7 \cdot 6H_2O$. The TG weight loss in the first stage (17.98 %), due to the elimination of 4 water molecules is close to the calculated value 18.02 %. It is related to the endothermic peak at 139 °C. The second weight loss (10.98 %), related to the endothermic peak observed at 365 °C, is compatible with theoretical loss of two water molecules (10.99 %), which corresponds to the formation of an amorphous anhydrous form $Co_2P_2O_7$. The exothermic peak in the range 575– 624 °C, with maximum rate observed at 592,8 °C is due to the crystallization of the amorphous diphosphate $Co_2P_2O_7$ [7].

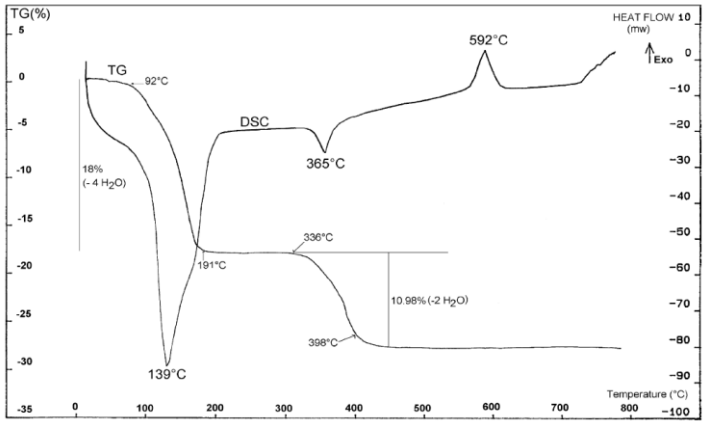

Figure 5. TG and DSC curves from $Co_2P_2O_7 \cdot 6H_2O$ [7].

The TG curve of Ni(II) diphosphate precursors indicates the thermal decomposition of NNPO ($NH_4NiPO_4 \cdot H_2O$) below 800 °C with two stages of weight loss. The first one occurs in a temperature range of 250-350°C, showing the weight loss of 21.47 and 1.95 % due to the dehydration of water and other volatile materials. Another one appears at 450-470 °C, which can be ascribed to the decomposition of inorganic mass from precursors in NNPO structure. However, the clear plateau formed above 470 °C indicates the formation of $Ni_2P_2O_7$ phase. In addition, both of the DTG (black line) and DTA (blue line) curves of NNPO show two main exothermic peaks at 316.67 °C, which can be attributed to the evolution of water vapor. Above 500 °C, these DTG and DTA curves show no significant change, indicating the formation of $Ni_2P_2O_7$ phase around this temperature [8].

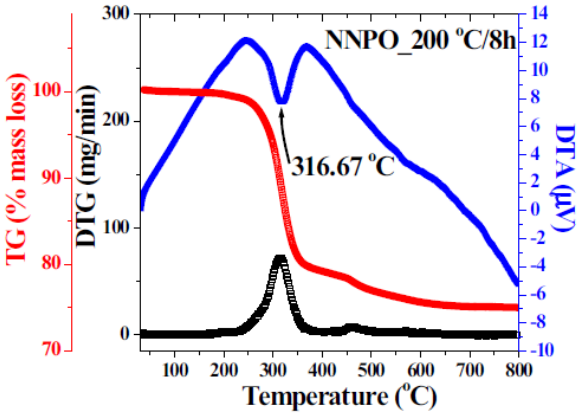

Figure 6. Thermal decomposition of nickel diphosphate precursor [8].

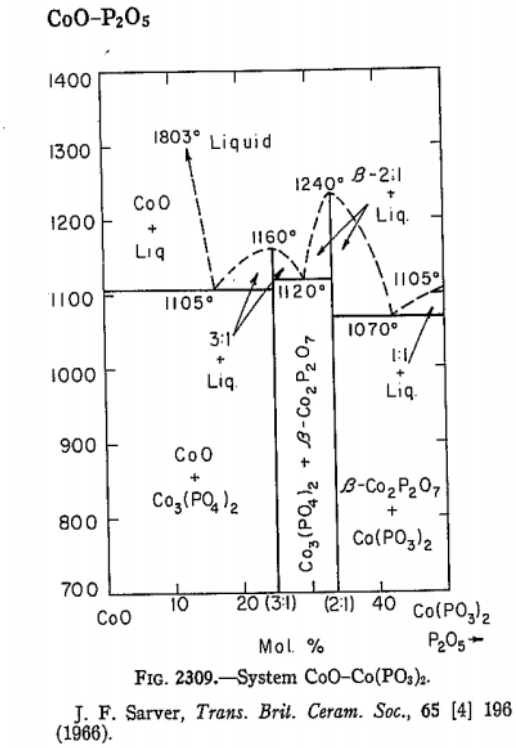

FIG. 2309.—System CoO–Co(PO$_3$)$_2$.

J. F. Sarver, *Trans. Brit. Ceram. Soc.*, 65 [4] 196 (1966).

Figure 7. Phase diagram for the system CoO-P_2O_5 [9]

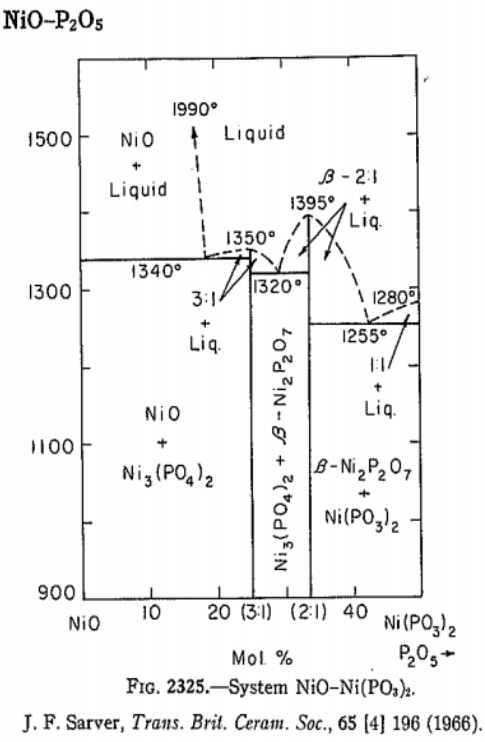

FIG. 2325.—System NiO–Ni(PO$_3$)$_2$.

J. F. Sarver, *Trans. Brit. Ceram. Soc.*, 65 [4] 196 (1966).

Figure 8. Phase diagram for the system NiO-P_2O_5 [9]

Orthophosphates and diphosphates are more stables than nitrates and sulphates. The melting point in $Co_3P_2O_8$ compound is 1160 °C and in the $Co_2P_2O_7$ compound is 1240 °C (Figure 7). The melting point in $Ni_3P_2O_8$ compound is 1350 °C and in the $Ni_2P_2O_7$ compound is 1395 °C (Figure 8). Thus, the temperature to use these compounds is higher.

Cobalt (II) phosphate and nickel (II) phosphate present quite similar catalytic activity and can be useful. But the combine of both metals results in a much powerful catalyst. It is logic to thick that in the upcoming future, new studies will focus in bimetallic or trimetallic catalysts instead of monometallic catalysts.

3.2. Coloration of compounds

The colour of Co(II) nitrates and Co(II) sulphates is red. It is attributed to octahedral coordination of Co(II) ions that are isolated or form chains in these structures. The colour of Ni(II) nitrates and Ni(II) sulphates is green. The Ni(II) ions are in octahedral site in them.

Blue colour is usually attributed to tetrahedrally coordinated Co^{2+} ions, and it can change depending on the hydration state, moving from pink colour in the octahydrate form to violet colour in the anhydrous form. Purple and violet compounds are obtained due to the presence of the Co(II) ions occupy octahedral positions and square-based pyramid positions in diphosphate and orthophosphate structures. Yellow colour in Ni(II) phosphates is attributed to six-coordinated Ni^{+2}. Strong charge-transfer transitions dominate the colour of these compounds [10].

Phosphates

P_2O_5 is included among the main glass-forming oxides together with SiO_2, B_2O_3 and GeO_2. Cations introduced from phosphates remain in glazed samples although partial or total dissolution of these structures occurs. Thus, the introduction of chromophore cations in materials originating from phosphates might have some advantages in the glass or ceramic industry because the oxygen ions in the first coordination of the cation may remain in the cooled liquid if the crystalline structure is not stable within the vitreous matrix [10].

Cobalt violet phosphate is included in the DMCA Classification of the Mixed Metal Oxide Inorganic Coloured Pigments. The colour of cobalt phosphate varies with its hydration State. Violet anhydrous cobalt phosphate, the tetrahydrate described as violet-pink or deep violet and the pink octahydrate are reported [10].

The blue colour of enamelled samples is attributed to Co^{+2} ions. Nickel ceramic pigments with a phosphate structure and solid solutions with a diphosphate and orthophosphate structure might also be useful as precursors of yellow ceramic pigments. Phosphate pigments exhibit a partial chemical and thermal stability and resistivity to dissolution agents, hence allowing their use as efficient colouring agent for coloration of ceramic glazes [10].

The colouring performance of cobalt pigments depends very much on their thermal stability, their chemical reactivity toward the glaze components and on the coordination of Co^{2+} ions (tetrahedral coordination is preferred to octahedral). The blue colour of enamelled samples has always been attributed to tetrahedrally coordinated Co^{2+} ions. The intense purple-blue obtained from enamelled $CoZr_4(PO_4)_6$ samples, for example, changes to blue depending on the composition of employed glaze. Ni^{2+} in sixfold coordination in oxides frequently produces green or yellow colouring. Bright yellow is the result of Ni^{2+} in a six-coordinated site significantly distorted from octahedral symmetry. Increased absorption intensity occurs when the metal ion d-d bands are in the proximity of an ultraviolet charge-transfer band. Strong charge-transfer transitions dominate the colour of some materials that contain Ni(II) [10].

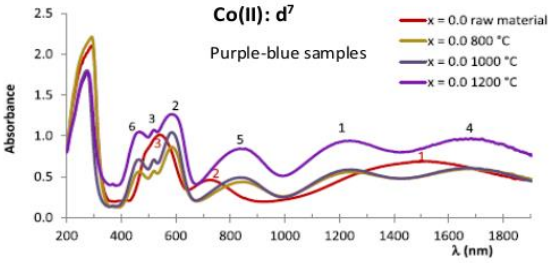

FIGURE 5 UV–vis–NIR spectra of $NH_4[CoPO_4]{\cdot}H_2O$ and $Co_2P_2O_7$ compounds ($x = 0.0$) fired at 800, 1000 and 1200°C. IC = 6 : (1) $^4T_1 \rightarrow {}^4T_2$, (2) $^4T_1 \rightarrow {}^4A_2$, (3) $^4T_1 \rightarrow {}^4T_1(P)$. IC = 5: (4) $^4A_2 \rightarrow {}^4A_1$, (5) $^4A_2 \rightarrow {}^4E$ (6) $^4A_2 \rightarrow {}^4E(P)$

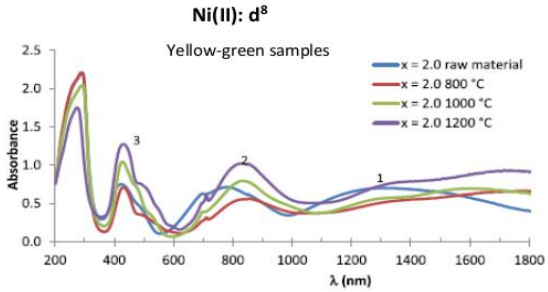

FIGURE 6 UV–vis–NIR spectra of $NH_4[NiPO_4]{\cdot}H_2O$ and $Ni_2P_2O_7$ compounds ($x = 2.0$) fired at 800, 1000 and 1200°C. IC = 6 : (1) $^3A_2 \rightarrow {}^3T_2(F)$, (2) $^3A_2 \rightarrow {}^3T_1(F)$, (3) $^3A_2 \rightarrow {}^3T_1(P)$

Figure 9. Visible spectrum of Cobalt (II), left, and Nickel (II), right [10].

Table 3. Colour variation of the $Co_{2-x}Ni_xP_2O_7$ compositions [10]

x	T (°C)	L*	a*	b*	Observed colour
0.0	180	51.38	+41.83	−34.16	Intense fuchsia pink
0.4	180	44.29	+31.31	−12.12	Deep reddish pink
0.7	180	53.71	+26.90	−3.78	Reddish pink
0.8	180	49.72	+27.33	−2.16	Reddish pink
0.9	180	51.72	+25.74	+0.17	Reddish pink
1.0	180	53.91	+24.06	+1.73	Reddish pink
1.2	180	57.25	+19.81	+7.57	Salmon-pink
1.3	180	59.83	+18.63	+8.00	Salmon-pink
1.6	180	68.13	+11.78	+17.82	Pink-beige
2.0	180	81.45	−12.18	+45.20	Yellowish green
0.0	1200	34.84	+11.53	−11.41	Intense violet
0.4	1200	39.84	+5.55	+0.01	Greyish violet
0.7	1200	45.60	+3.66	+4.25	Greyish violet
0.8	1200	45.49	+2.81	+6.40	Reddish violet
0.9	1200	43.08	+3.24	+9.95	Reddish brown
1.0	1200	41.05	+3.99	+11.64	Reddish brown
1.2	1200	52.00	+1.35	+16.62	Beige
1.3	1200	46.50	+3.57	+18.55	Beige-brown
1.6	1200	59.62	+2.15	+27.42	Yellowish
2.0	1200	71.39	+17.54	+55.52	Intense yellow

This table shows how colour varies in a $Co_{2-x}Ni_xP_2O_7$ compound. When there is no Nickel, the compound is intense fuchsia pink; however, as the amount of nickel increases, compound acquires a yellow Touch, ending with a yellowish green colour when there is no Cobalt.

3.3. Conductivity

Divalent metal ions are among the major inorganic species in natural waters and are also of practical importance as they have significant biological functions. Their hydrated cations tend to behave as weak acids [11].

Sulphates

Table 4. Conductivities of $CoSO_4$ and $NiSO_4$ in water [10].

$\tilde{m}$ (10^3)	T=278.15	T=283.15	T=288.15	T=293.15	T=298.15	T=303.15	T=308.15
$CoSO_4$, D=0.1590							
0.22001	73.723	84.867	96.782	109.245	122.080	135.415	149.386
0.46111	70.273	80.956	92.149	103.861	116.083	128.626	141.632
0.70703	67.766	78.033	88.771	100.029	111.633	123.703	135.807
0.93856	65.939	75.885	86.340	97.214	108.443	119.866	131.769
1.1744	64.334	74.014	84.186	94.774	105.581	116.855	128.401
1.4078	62.941	72.426	82.324	92.601	103.212	114.185	125.428
1.6993	61.409	70.630	80.265	90.295	100.644	111.297	122.167
1.9875	60.116	69.092	78.522	88.303	98.414	108.773	119.376
2.3530	58.649	67.412	76.581	86.149	95.947	106.046	116.290
2.7029	57.439	66.059	75.017	84.309	93.900	103.729	113.717
3.1092	56.200	64.618	73.370	82.470	91.815	102.163	111.086
3.5193	55.086	63.305	71.860	80.785	89.914	99.231	108.754
$NiSO_4$, D=0.1644							
0.26418	73.036	84.135	95.866	108.156	120.986	134.275	148.014
0.54623	69.449	79.977	91.052	102.639	114.720	127.166	139.720
0.84764	66.585	76.670	87.260	98.331	109.781	121.575	133.744
1.1650	64.268	73.959	84.160	94.771	105.734	117.104	128.705
1.4957	62.305	71.688	81.552	91.787	102.416	113.330	124.526
1.8325	60.633	69.779	79.326	89.266	99.566	110.146	120.940
2.2184	59.007	67.896	77.182	86.830	96.787	107.032	117.486
2.5906	57.621	66.290	75.343	84.744	94.461	104.398	114.572
3.0007	56.334	64.792	73.632	82.792	92.256	101.960	111.815
3.4238	55.170	63.428	72.069	81.028	90.276	99.672	109.154

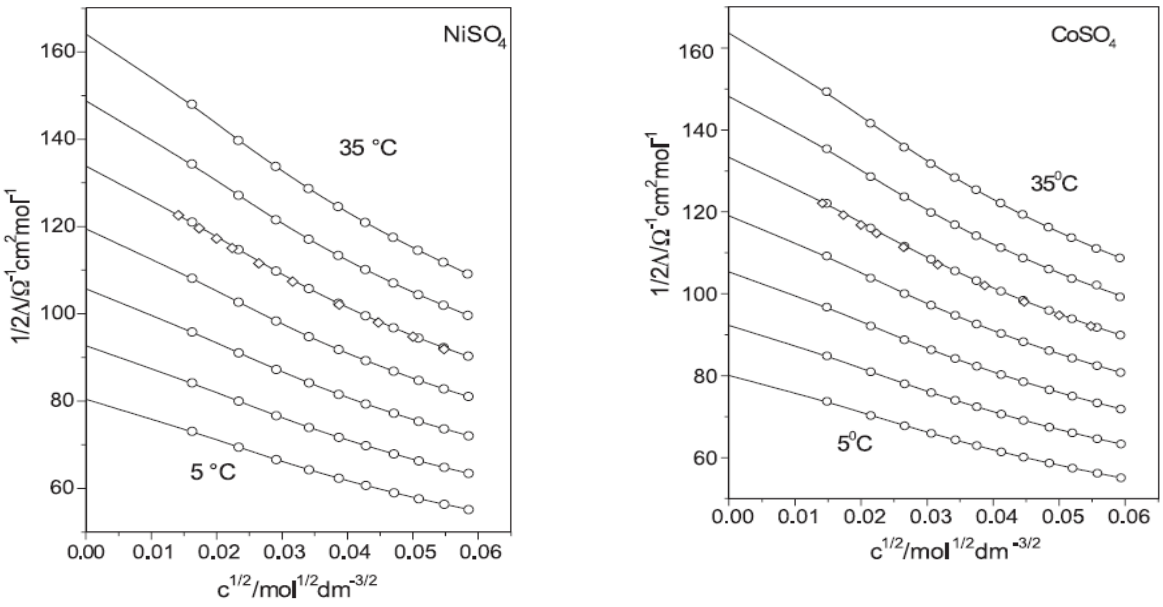

Figure 10. Representations of the conductivities de $NiSO_4$ (left) and $CoSO_4$ (right) at different temperatures [11].

In bibliography, conductivities were determined with the help of a three-electrode measuring cell described elsewhere. The cell was calibrated by potassium chloride solution. At the beginning of every measuring cycle, the cell was filled with a weighed amount of water. After measurement of the solvent conductivity at all temperatures of the program, weighed amounts of a stock solution were added using a gas-tight syringe and the temperature program was repeated [11].

Table 5. The table on the left shows limiting equivalent conductivities and the table on the right shows the conductivity of the ions separately [11].

T	$1/2\Lambda^{\infty}$	K_A (I: n=1)	R (J_2)	$1/2\Lambda^{\infty}$	K_A (II: n=2)	R (J_2)
			$MgSO_4$[b]			
		R=0.616			R=0.896	
278.15	79.57	115.6	0.477	79.68	144.6	0.882
283.15	91.83	117.4	0.484	91.96	146.9	0.887
288.15	104.74	118.8	0.504	104.89	148.7	0.900
293.15	118.28	121.5	0.501	118.46	152.0	0.899
298.15	132.50	126.0	0.498	132.70	157.2	0.899
303.15	147.43	133.6	0.466	147.66	165.5	0.882
308.15	163.10	144.7	0.393	163.37	177.6	0.842
			$CoSO_4$			
		R=0.620			R=0.900	
278.15	79.94	153.7	0.542	80.05	182.9	0.916
283.15	92.14	154.7	0.559	92.26	184.3	0.929
288.15	105.18	161.3	0.536	105.33	191.5	0.915
293.15	118.90	169.5	0.492	119.07	200.5	0.889
298.15	133.11	176.6	0.470	133.31	208.3	0.877
303.15	147.96	187.4	0.337	148.19	220.1	0.806
308.15	163.37	195.2	0.422	163.64	228.4	0.853
			$NiSO_4$			
		R=0.620			R=0.885	
278.15	80.18	162.3	0.454	80.30	192.1	0.868
283.15	92.43	163.0	0.474	92.57	193.3	0.881
288.15	105.43	166.5	0.476	105.59	197.3	0.883
293.15	119.12	171.7	0.469	119.30	203.1	0.880
298.15	133.48	179.0	0.444	133.69	211.2	0.867
303.15	148.34	185.4	0.470	148.58	217.7	0.878
308.15	163.61	189.9	0.495	163.88	223.4	0.900

T	λ^{∞} ($1/2Mg^{2+}$)[b]	λ^{∞} ($1/2Co^{2+}$)	λ^{∞} ($1/2Ni^{2+}$)
278.15	33.61	34.05	34.30
283.15	38.28	38.58	38.89
288.15	43.08	43.52	43.78
293.15	47.99	48.60	48.83
298.15	53.03 53.06[c]	53.64	54.02
303.15	58.18	58.72	59.11
308.15	63.47	63.74	63.90

Diphosphates

In Co(II) diphosphate, two different regions such as potential-dependant and potential-independent areas were seen in the CV (cyclic voltammetry) curve. Since the area under the redox peaks (potential-dependant area) was higher, a prominent faradic type of charge storage mechanism has been carried out using the multivalent cobalt ions from the framework. In both reduction and oxidation peaks, a slight shift is observed at a higher scan rate which may be assigned to the internal resistance, sluggish ion mobility and less transfer kinetics of the battery type active electrode (figure on the right). Besides, considering the anodic peak, the cathodic peak was not the mirror image of the other at slightly higher scan rates which may be assigned to significant irreversibility in faradic reaction because of ohmic and polarization effect during redox process [12].

A comparative CV curve (figure on the left) of samples prepared at different calcination temperatures shows that the sample prepared at the higher temperature (C-750) possesses the good capacitance which may be because of improved active sites and prominent spacing which might favour an enhanced electrochemical performance. A raise of peak current with an increase in scan rate portrays its dependency on the scan rate [12].

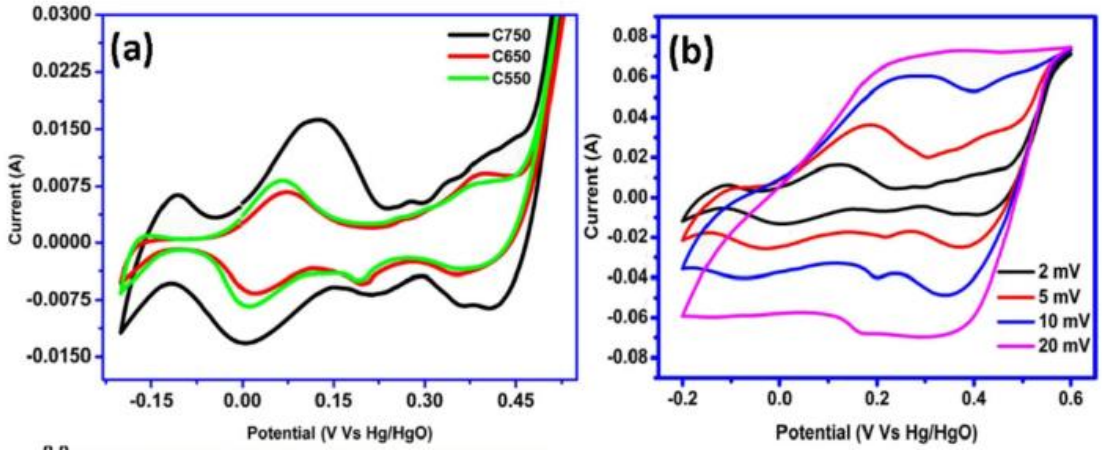

Figure 11. CV curves of $Co_2P_2O_7$ electrodes (left) and C-750 curves at different currents [12].

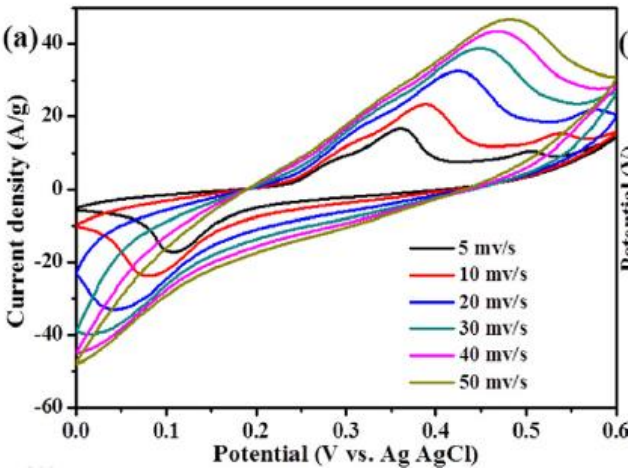

Figure 12. CV curve of $Ni_2P_2O_7$ [13].

The shapes of CV curves are quite different from those of electric double layer capacitors. Compared with the zero current line, the CV diagram has the shape of rectangle and mirror, which indicates that it has superior capacitance characteristics and fast charging/discharging rate. Because of the reaction of Ni^{+2} and Ni^{+3} on the surface of $Ni_2P_2O_7$ electrode material, the CV curve consists of a pair of significant redox peaks. The CV curves consisting of a pair of vital redox peaks is due to the reaction of Ni^{2+} with Ni^{3+} on the surface of $Ni_2P_2O_7$ electrode material. It was found that the redox peak shifted to higher and lower potentials. The large potential separation is mainly attributed to the resistance of the electrodes [13].

3.4. Magnetism

The magnetism of a material is directly related to the number of electron spins. For example, when there is the same amount of electron spins in opposite directions, the magnetism of this material is cancelled. Having in mind electronic distribution in valence orbitals, both cobalt (Z = 27) and nickel (Z=28) have most electron spins in the same direction, so they are strongly magnetic. Many phosphates obey the Curie-Weiss Law especially at high temperatures. They are paramagnetic substances. At temperatures lower than the Néel point, T_N, the electron spins are aligned antiparallel and behave like antiferromagnetic substances.

Orthophosphates

The magnetic measurements of the $Ni_3(PO_4)_2$ compound were recorded in the FC (field cooled) and ZFC (zero field cooled) modes using a Quantum Design MPSM-7 magnetometer at values of 0.1, 0.05 and 0.01T. A maximum in the molar magnetic susceptibility is observed at 17.1K indicating the existence of 3D antiferromagnetic interactions in good agreement with the structural data. From the magnetic measurements performed at different magnetic fields, it was observed that the thermal evolution of the molar magnetic susceptibility does not show any irreversibility at low temperatures indicating a purely antiferromagnetic behaviour of $Ni_3(PO_4)_2$. The values of the Curie and Curie–Weiss constants, 4.08 cm^3Kmol^{-1} and θ=-33.3K, respectively. The g-value obtained from the Curie constant in the paramagnetic region is g= 2.33, characteristic of Ni(II) cations in octahedral geometry. The effective magnetic moment calculated from the Curie constant is 3.29μB, in the range habitually found for the Ni(II) (d^8) cations. The $\chi_m T$ vs T curves decreases from 3.66 cm^3Kmol^{-1} at room temperature to 0.28 cm^3Kmol^{-1} at 5K, in good agreement with the existence of antiferromagnetic interactions [14].

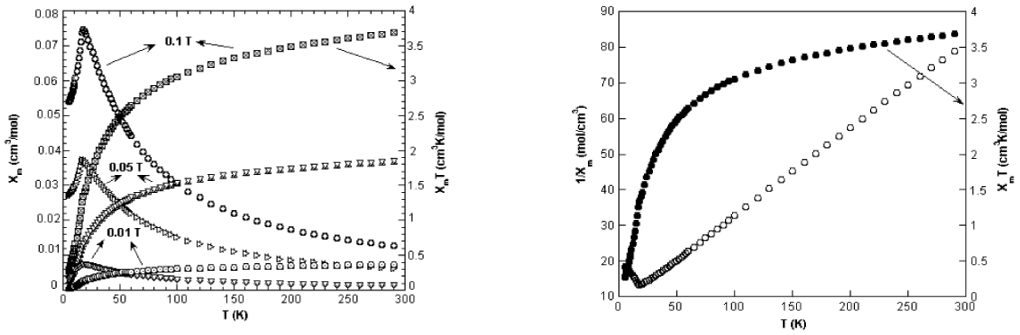

Figure 13. $\chi_m T$ vs T curves.

Diphosphates

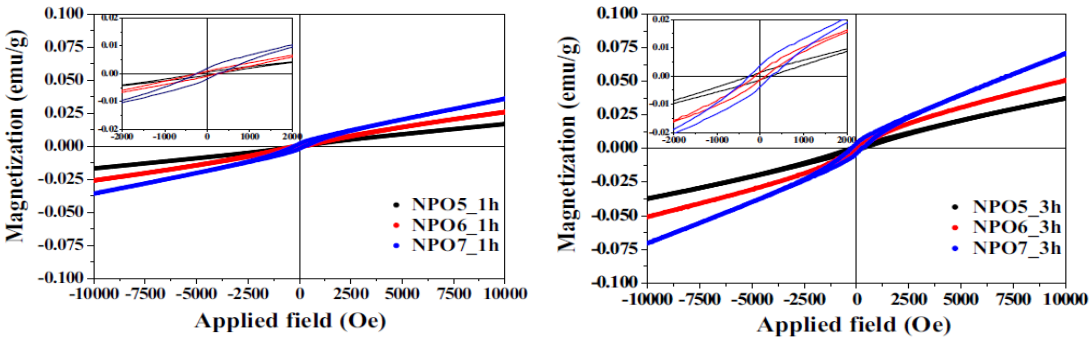

Figure 14. M-H curves for calcined samples for one hour (left) and three hours (right).

The M–H curves of all NPOs (nickel phosphate) calcined at different temperatures for 1h and 3h are shown. It can be seen in left figure that the M–H curves of all NPOs_1 h display very small and narrow loops with unsaturated magnetizations, indicating the weak ferromagnetic behaviour. In the case of NPOs calcined for 3 h, these samples behave in a similar way with the larger hysteresis loops, higher unsaturation magnetizations (*M*) and coercivity (H_c) as shown in right figure. It is suggested that the weak ferromagnetic behaviour in these samples is due to the calcination process that result the distortion of crystal structure and the increasing of particle size. The *M* at 10 kOe, and *Hc* values of all NPOs are summarized in Table 6. Moreover, it is obviously seen in Table 6 that the increase of calcination temperature and time can result in the enhancement of *M* and *Hc* values, because of the increase of particle size [8].

Table 6. Magnetization values.

Parameters		NPOs_1 h			NPOs_3 h		
		NPO5	NPO6	NPO7	NPO5	NPO6	NPO7
M at 10 kOe		0.0166	0.0266	0.0358	0.0373	0.0516	0.0715
H_c		126.715	149.688	204.833	241.164	180.083	349.272
Csc ($F\ g^{-1}$)	1 A g^{-1}	794.457	905.687	548.356	737.867	653.332	416.667
	1.5 A g^{-1}	750.590	853.454	516.464	696.465	600.765	390.231
	2 A g^{-1}	705.752	812.324	488.644	645.777	552.746	367.654
	3 A g^{-1}	630.644	730.256	426.979	576.743	483.614	316.852
	4 A g^{-1}	551.113	646.970	382.753	501.113	426.425	275.855
	6 A g^{-1}	406.643	506.930	279.006	370.077	320.936	200.900
	8 A g^{-1}	307.847	392.302	213.432	280.370	256.635	140.865
	10 A g^{-1}	231.953	296.530	141.113	195.353	183.332	76.536
Retention (%)		86.24	90.80	83.26	76.48	74.00	64.94
Rs (Ω)		0.716	0.835	0.731	0.918	0.892	0.932
Rct (Ω)		2.159	1.804	2.455	2.154	2.698	2.588
Zw		4.878	4.855	4.640	3.565	3.737	3.144

4. CONCLUSIONS

Nitrates

As it has been studied in point two, both $Co(NO_3)_2$ and $Ni(NO_3)_2$ present a trigonal symmetry, where the main ions occupy octahedral positions and isolated octahedral are bound by nitrate ions. Moreover, the atoms are distributed in an equal form inside the structure, so we can conclude that these structures are isostructural. However, $Ni(NO_3)_2$ also can present a cubic symmetry, which is completely different to the trigonal one.

Anhydrous transition metal nitrates and their hydrates are widely used for preparation of catalyst materials such as oxides and metals, and it is no surprise that both cobalt(II) nitrate and nickel(II) nitrate are excellent catalyst. They are transition metals, Co (Z = 27) and Ni (Z = 28), and they have multiple electrons in valence shell (d-orbital). Both of them show great capacity to lend and withdraw electrons from the reagents, while they also can interchange their oxidation. To sum up, we can conclude that both cobalt(II) nitrate and nickel(II) nitrate are isostructural and have the perfect characteristics to be excellent catalysts.

Sulphates

Cobalt(II) sulphate and nickel(II) sulphate present an isostructural polymorph, which is the beta form. This one shows an orthorhombic symmetry, where the main ions occupy octahedral positions and the octahedral share edges forming chains of octahedra. While nickel(II) sulphate has only shown a polymorph, almost three of them can be distinguished for cobalt(II) sulphate. At low temperatures, $CoSO_4$ crystallizes in beta-form, like nickel(II) sulphate; however, when increasing the temperature (above 432^{o}C) a new stable phase is formed, the alpha form. The new gamma-form appears when increasing the pressure. By now, it has not been isolated and proper structural studies are needed in the coming future.

The most important property for cobalt(II) and nickel(II) sulphates is the conductivity. The conductivity of cobalt(II) sulphate and nickel(II) sulphate are very similar. Moreover, the study of the conductivity of isolated cobalt (II) and nickel (II), also reveals that the difference between these two ions is very small. The conductivity behaviour of cobalt (II) and nickel (II) is very similar and there are no significant differences between them two.

Phosphates

As said in the introduction, phosphates include diphosphates, $M_2P_2O_7$, and orthophosphates, $M_3P_2O_7$ where M = Co, Ni. In both cases, cobalt(II) and nickel(II) are isostructural.

In first place, diphosphates can show as an alpha polymorph, with a monoclinic symmetry, where the divalent ions occupy octahedral positions, and as a beta polymorph, with an orthorhombic symmetry, where the divalent ions occupy octahedral positions. Both cobalt(II) and nickel(II) have shown these polymorphs.

On the other hand, orthophosphates show a unique structure, which includes a monoclinic symmetry where divalent ions occupy octahedral positions. Like the previous structure, both cobalt(II) and nickel(II) show this structure. Moreover, cobalt(II) orthophosphate also presents a metastable phase, which is very similar to the stable one. More studies on this one are needed in the future.

One of the most important characteristic of phosphates is the coloration of compounds. As studied, blue colour is attributed to tetrahedrally coordinated Co^{2+} ions and yellow colour is typically from the six-coordinated Ni^{+2}. However, this colouring performance depends on the thermal stability, the chemical reactivity toward the glaze components and on the coordination of the ions.

The other interesting point is the ferromagnetic behaviour. Both cobalt (d^7) and nickel (d^8) present many electron spins in the same direction in the valence shell, which is a clear characteristic of ferromagnetic materials. However, as it has been studied, cobalt and nickel phosphates (diphosphates and orthophosphates) show an antiferromagnetic behaviour. Phosphates are paramagnetic substances, so the antiferromagnetic behaviour is studied by the Curie-Weiss law. According to this law, when the temperature increases, the magnetization of a paramagnetic material decreases. This law affirmation is in good concordance with the published results.

5. BIBLIOGRAPHY

[1] Inorganic Crystal Structure Database (ICSD). *Fachinformation-szentrum.* Karlsruhe, Germany: FIZ; 2014.

[2] *https://www.ecured.cu/Catalizador*

[3] W. Brockner, C. Ehrhardt, M. Gjikaj, Thermochimica Acta 456 (2007) 64-68.

4. W. Brockner, C. Ehrhardt, M. Gjikaj, Thermochimica Acta 432 (2005) 36-40.

5. B. Jankovic, S. Mentys, D. Jelic, Physica B 404 (2009) 2263-2269.

6. B. Senthilkumar, A. Irshad, P. Barpanda, ACS Appl. Mater. Interfaces 2019, 11, 33811-33818.

7. M.Harcharras, A. Ennaciri, F. Capitelli, G. Mattei, Vibrational Spectroscopy 33 (2003) 189-196.

8. A. Karaphun, S. Maensiri, E. Swatsitang,Journal of Materials Science: Materials in Electronics 2019) 30:3019-3031.

9. J. F. Sarrer, Trans. Brit. Ceram. Soc., 65 [4] 196 (1966).

10**.** MA. Tena, R. Mendoza, C. Trobajo, J. R. García, S. García-García, J Am Ceram Soc. 2019; 102:3695-3704.

11. M. Bester Rogac, V. Babic, T.M. Perger, R. Neueder, J. Barthel, Jornal of Molecular Liquids 118 (2005) 111-118.

12. P. Matheswaran, P. Karuppiah, P. Thangavelu, DE part of Springer Nature 2021.

13. Zhou Y., Liu C., Li X., Sun L., Wu D., Li J., Huo P., Wang H., Journal of Alloys and Compounds 790 (2019) 36-41.

14. J. Escobal, J.L. Pizarro, J.L. Mesa, J.M. Rojo, B. Bazan, M.I. Arriortua, T. Rojo, Journal of Solid State Chemistry 178 (2005) 2626-2634.